Available online at www.sciencedirect.com
ScienceDirect
Journal of the European Ceramic Society 29 (2009) 2595–2601
www.elsevier.com/locate/jeurceramsoc

Effects of $Bi_4Ti_3O_{12}$ addition on the microstructure and dielectric properties of modified $BaTiO_3$ under a reducing atmosphere

T.A. Jain *, C.C. Chen, K.Z. Fung

Department of Materials Science and Engineering, National Cheng Kung University, Tainan 701, Taiwan, ROC

Received 12 November 2008; received in revised form 14 February 2009; accepted 26 February 2009
Available online 26 March 2009

Abstract

The effects of $Bi_4Ti_3O_{12}$ addition on the microstructure and dielectric properties of Mn-modified $BaTiO_3$ were investigated to develop low temperature fired $BaTiO_3$-based ceramics with stable temperature characteristics. The sintering temperature of Mn-doped $BaTiO_3$ could be reduced to 1200 °C by adding more than 1 mol% $Bi_4Ti_3O_{12}$. TEM results show an apparent core–shell structure with 2 mol% $Bi_4Ti_3O_{12}$ addition. However, it was destroyed when the $Bi_4Ti_3O_{12}$ content increased from 2 to 4 mol%. The permittivity decreased and the Curie temperature shifted to higher temperature when the $Bi_4Ti_3O_{12}$ content increased from 0 to 3 mol%. The temperature characteristic of capacitance was very close to the EIA X8R specification when 2 mol% $Bi_4Ti_3O_{12}$ was added due to the presence of the core–shell grain structure and raised Curie temperature. With adequate $Bi_4Ti_3O_{12}$ addition, the $BaTiO_3$-based system shows great potential for applications in EIA X8R-type multilayer ceramic capacitors.

Keywords: Grain growth; Electron microscopy; Dielectric properties; $BaTiO_3$

1. Introduction

$BaTiO_3$-based materials with high dielectric properties are important due to their use in multilayer ceramic capacitors (MLCCs) in the electronic components. X7R and X8R specifications were established for different applications of MLCCs. (X7R: the capacitance in the temperature range of −55 to 125 °C is within ±15% of room temperature capacitance; X8R: the capacitance in the temperature range of −55 to 150 °C is within ±15% of room temperature capacitance). In the automobile industry, the engine electronic control unit (ECU), programmed fuel injection (PGMFI), and anti-lock brake system (ABS) all use MLCCs at higher temperatures, especially ECU, which is placed in the engine compartment. MLCCs in these control modules must satisfy X8R specifications to maintain their performance at higher temperatures.

The Curie temperature (T_C) of a $BaTiO_3$ crystal is around 125 °C. This intrinsic limit is the reason why the X8R specification is difficult to meet for $BaTiO_3$-based materials. The densification of $BaTiO_3$ has been proved to be very slow. Thus, the sintering temperatures as high as 1300 °C are required for $BaTiO_3$.[1,2] In order to solve both problems, certain dopant oxides are mixed with $BaTiO_3$. To obtain a moderate temperature coefficient of capacitance (TCC), rare-earth elements (Tm, Pr, Gd, Ho, Er, Yb, and Lu) have been introduced to $BaTiO_3$-based dielectrics with base metal electrodes (BMEs) in the fabrication of MLCCs.[3,4] It was found that doped rare-earth elements with larger ionic radii (Pr, Gd) caused the T_C of the examined system to be lower than those doped with ions of smaller ionic radii (Yb, Lu). The ionic radius of rare-earth elements plays an important role on the temperature coefficient of capacitance; the addition of rare-earth elements with smaller ionic radii leads to an improvement in the temperature dependence of dielectric properties.[5–10] Lin et al.[11] found that the densification process of $BaTiO_3$-based ceramics is commonly accelerated by introducing excess TiO_2 or BaO into the system lattice. Chen et al.[12] reported that in the sintering process of $BaTiO_3$ with excess SiO_2, the formation of a liquid phase enhances the cation diffusion via dissolution and reprecipitation processes.

Recently, two bismuth titanate compounds, $Na_{0.5}Bi_{0.5}TiO_3$ and $K_{0.5}Bi_{0.5}TiO_3$, with a perovskite structure and a relatively high T_C have been used to raise the T_C of $BaTiO_3$[13,14]. $Bi_4Ti_3O_{12}$ is another bismuth titanate that received attention. M'Peko et al.[15] studied the densification process of $Bi_4Ti_3O_{12}$ (BIT)-doped

* Corresponding author. Tel.: +886 65108800; fax: +886 63840035.
E-mail addresses: tajain@xuite.net, ta.jain@darfon.com.tw (T.A. Jain).

0955-2219/$ – see front matter © 2009 Elsevier Ltd. All rights reserved.
doi:10.1016/j.jeurceramsoc.2009.02.015

$BaTiO_3$ compounds, and reported that 90% of the theoretical density could be achieved with 2% BIT after sintering at 1100 °C for 2 h. BIT has a typical perovskite structure and a very high T_C of 675 °C.[16] It is an attractive material for increasing T_C of $BaTiO_3$. Most MLCCs using BMEs, such as nickel and copper, must be fired at a low oxygen partial pressure to avoid BME oxidation, which leads to the presence of semiconducting properties in $BaTiO_3$ due to the reduction of Ti ions. Therefore, Mn^{2+} ions, acting as acceptors at the Ti sites of the $BaTiO_3$ lattice, are widely used to prepare non-reducible $BaTiO_3$ ceramics.[17,18] In this paper, we investigated the influence of $Bi_4Ti_3O_{12}$ on the macro/microstructure and the dielectric properties of 1% Mn-doped $BaTiO_3$, i.e. $Ba(Ti_{0.99}Mn_{0.01})O_3$, which was sintered under a reducing atmosphere. The variation of T_C is used to estimate the application of the investigated ceramic material in X8R-type MLCCs.

2. Experimental procedure

BIT was prepared using a conventional solid-state reaction with Bi_2O_3 (Alfa Aesar, 99%) and TiO_2 (Riedel-de Haën, 99%) as starting materials. The stoichiometric powders were mixed in a ball mill for 12 h and then dried at 100 °C for 24 h. Commercial $BaTiO_3$ powder with a mean particle size of 0.3 μm was mixed with various amounts of BIT (0, 1, 2, 3, and 4 mol%) and 1 mol% reagent-grade Mn_3O_4. The mixtures were homogenized by ball milling for 24 h. After drying at 100 °C for 24 h, the mixtures were uniaxially pressed into discs under 200 MPa. Sintering was conducted at 1200 °C for 4 h under a reducing atmosphere of 1% H_2 + 99% N_2. Reoxidation of the ceramic specimens was carried out at 900 °C for 2 h in a nitrogen atmosphere.

Crystal structure of the samples were identified at room temperature using an X-ray diffractometer (XRD; Model: D-MAX IIIV, Rigaku Co., Tokyo, Japan) with Cu Kα radiation, operated at 30 kV, 20 mV, and a scanning rate of 1° min^{-1} within the range of 2θ from 20° to 80°. The lattice constants of samples were determined with the aid of silicon standard. Differential scanning calorimetry (DSC; Model: DSC131, Setaram, France) was used to determine the T_C of the samples.

The density of the sintered samples was measured using the Archimedes method. Except for the pure $BaTiO_3$ sample, the sample densities were identified as being higher than 95% of the theoretical density. The polished and as-fired surfaces of the sintered samples were observed using a scanning electron microscope (SEM; Model: S-3000, Hitachi, Japan). The microstructure of the samples was examined with a transmission electron microscope (TEM; Model: JEM-3010) equipped with an energy dispersive X-ray spectroscope (EDS).

In order to measure the sample's electrical properties, copper electrodes were attached to the surface of the sintered discs and fired at 900 °C for 10 min. Dielectric permittivity and the dissipation factor of the disc-type capacitors were measured using an impedance analyzer (Model: Agilent HP4284A) in a temperature range of −55 to 150 °C at 1 kHz and 1 V_{rms}. Insulation resistance (IR) was measured using a high resistance meter (Model: Agilent HP4339B) at room temperature; the applied voltage was 10 V_{DC} and the charging time was 60 s.

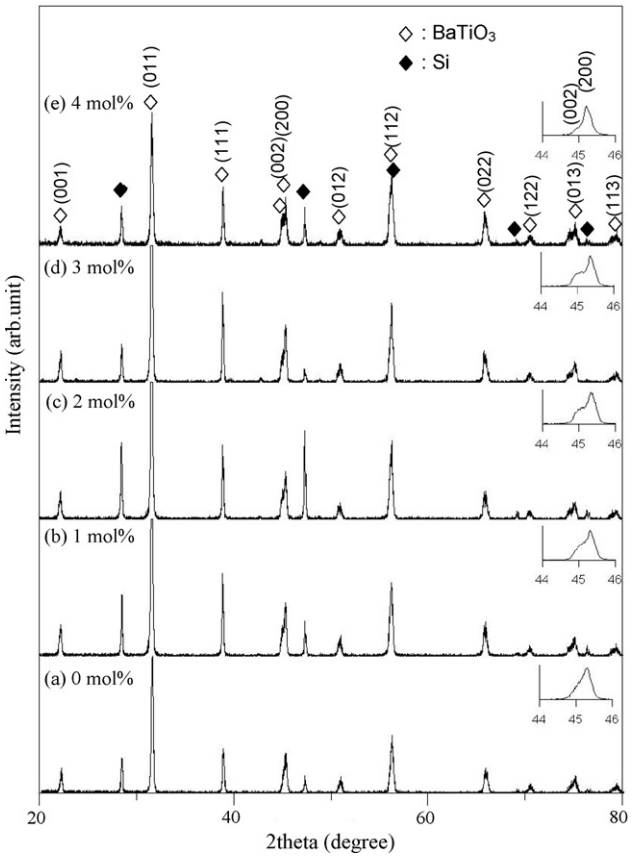

Fig. 1. XRD patterns of $Ba(Ti_{0.99}Mn_{0.01})O_3$ ceramics as a function of $Bi_4Ti_3O_{12}$ content: (a) 0 mol%, (b) 1 mol%, (c) 2 mol%, (d) 3 mol% and (e) 4 mol%.

3. Results and discussion

Fig. 1 illustrates the XRD patterns of the $Ba(Ti_{0.99}Mn_{0.01})O_3$ ceramics with various amounts of BIT content that were sintered at 1200 °C for 4 h under a reducing atmosphere. Except for the diffracted reflection from the silicon standard, no secondary phase was observed. For samples containing 0–4 mol% BIT, a single perovskite phase was observed. The solubility of BIT in $Ba(Ti_{0.99}Mn_{0.01})O_3$ is more than 4 mol%. The tetragonality of samples was examined based on the (0 0 2) and (2 0 0) reflections. From Fig. 1(a), pure $Ba(Ti_{0.99}Mn_{0.01})O_3$ shows separation of (0 0 2) and (2 0 0) peaks when 2θ range was scanned between 44° and 46°. This result indicates that the $Ba(Ti_{0.99}Mn_{0.01})O_3$ exhibits tetragonal structure with lattice parameters $a = 4.0132$ Å, $c = 4.0193$ Å. The (0 0 2) and (2 0 0) reflections remained separated up to 2–3 mol% of BIT doping. Finally, these two reflections merged due to the elimination of tetragonality in 4 mol% BIT-doped $Ba(Ti_{0.99}Mn_{0.01})O_3$. Thus, it is reasonable to expect that 4 mol% BIT-doped $Ba(Ti_{0.99}Mn_{0.01})O_3$ has lower capacitance.

The effect of the BIT content on the unit cell of $Ba(Ti_{0.99}Mn_{0.01})O_3$ estimated from Fig. 1 is shown in Fig. 2. The unit cell volumes of the perovskite phases were determined using the method of indexing and calculation with the least-squares powder diffraction program – unit cell – written by Holland and Redfern,[19] in which silicon was used as an internal standard. In

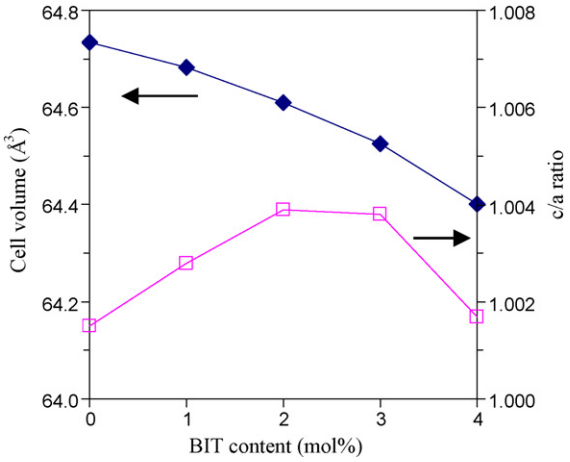

Fig. 2. Changes in unit cell volume and *c*/*a* ratio of $Ba(Ti_{0.99}Mn_{0.01})O_3$ ceramics with an increase of $Bi_4Ti_3O_{12}$ content.

Fig. 2, with an increase of BIT content, the volume of a unit cell decreases almost linearly from 64.7339 to 64.4008 $Å^3$. The decrease of the unit cell volume resulting from BIT doping is due to the occupation of smaller Bi^{3+} ions (1.02 Å) at the Ba^{2+} sites of $Ba(Ti_{0.99}Mn_{0.01})O_3$. This linear relationship also implies that up to 4 mol% of BIT has completely incorporated into the ABO_3 lattice; therefore, no second phase is present in Fig. 1.

The degree of tetragonality can be quantified by the *c*/*a* ratio (*c* and *a* are the lattice parameters of tetragonal perovskite). The results in Fig. 2 show that the *c*/*a* ratio increases from 1.0015 to 1.0039 when the BIT content increases from 0 to 2 mol%. Then, the *c*/*a* ratio decreases from 1.0038 to 1.0017 when the BIT content increases from 3 to 4 mol%. As mentioned above, we found that the *c*/*a* ratio of 4 mol% BIT-doped $Ba(Ti_{0.99}Mn_{0.01})O_3$ is similar to that of undoped $Ba(Ti_{0.99}Mn_{0.01})O_3$. Accordingly, it is possible that, the change of T_C in this system is caused by the lattice mismatch between a undoped $Ba(Ti_{0.99}Mn_{0.01})O_3$ crystal region (core) and a Bi ion incorporated region (shell) inducing an internal stress model that suppresses the phase transition from tetragonality to cubic and increase tetragonality (*c*/*a* ratio).[5,7,8] The compound with 4 mol% BIT addition will exhibit a lower T_C because the effect of the internal stress resulting from the similar tetragonality of core and shell in grains is absent. In other words, 4 mol% BIT-doped $Ba(Ti_{0.99}Mn_{0.01})O_3$ may have no core–shell structures, as indicated by XRD results.

The dielectric properties of ceramic materials are strongly affected by their microstructual characteristics. In this work, the macrostructural characteristics were determined by observing the changes of the materials' relative densities and from SEM micrographs. Fig. 3 shows the relative density of $Ba(Ti_{0.99}Mn_{0.01})O_3$ ceramics as a function of the BIT content. The relative density of $Ba(Ti_{0.99}Mn_{0.01})O_3$ without BIT is much lower than those of the other samples under a heat treatment of 1200 °C for 4 h. This low relative density (around 85%) is consistent with the reports of Hshie and Fung[2] and Lin et al.[11] that the densification rate of $BaTiO_3$ is very slow, and temperatures above 1300 °C are needed for sintering. According to the study of M'Peko et al.[15], low relative density leads to poor dielectric properties. Thus, the densification of $BaTiO_3$

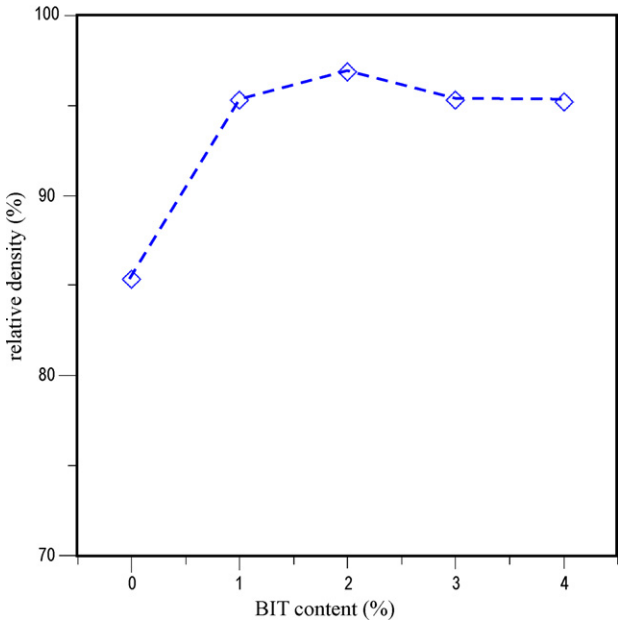

Fig. 3. Relative density of $Ba(Ti_{0.99}Mn_{0.01})O_3$ ceramics as a function of $Bi_4Ti_3O_{12}$ content.

needs to be enhanced for its applications in MLCCs. In Fig. 3, it was found that when 1 mol% BIT was added, the relative density of the sintered $Ba(Ti_{0.99}Mn_{0.01})O_3$ ceramic reached 95%. Since samples with 1–4 mol% BIT doping exhibited relative densities higher than 95%, the sintering temperature can be effectively reduced to 1200 °C due to liquid phase sintering that enhance the cation diffusion and sinterability. The densification of the BIT–$Ba(Ti_{0.99}Mn_{0.01})O_3$ system with relative density of 95–97% was achieved when heated at 1200 °C for 4 h. It was higher than those of the BIT–$BaTiO_3$ system under the conditions of 1200 °C for 2 h (85–94%) in the M'Peko et al. study,[15] perhaps due to Mn ion addition and the longer sintering time. Such a low sintering temperature reduces the shrinkage stress between ceramics and electrode material and power consumption in the MLCC manufacturing process.

Fig. 4 shows the SEM micrographs of polished and etched surfaces of the sintered samples doped with various amounts of BIT content. The grain size was significantly increased from 0.38 to 0.57 μm when the BIT content was increased. In agreement with M'Peko et al.,[15] the markedly large densification of 2–4 mol% BIT-doped $BaTiO_3$ is due to the formation of liquid phase after the reaction between $BaTiO_3$ and BIT. Yang et al.[20] also found that the densification and the grain growth processes both rely on mass transport. In other words, doping BIT into $Ba(Ti_{0.99}Mn_{0.01})O_3$ enhances the densification and the grain growth. Thus, the grain growth with the change of BIT content is closely related with the formation of liquid phases which enhance the cation diffusion in the system. From the study of Yamaoka et al.,[21] the liquid phase is $BaBi_4Ti_4O_{15}$ and its melting process occurs at 1050 °C. Due to the formation of $BaBi_4Ti_4O_{15}$ from the reaction between $BaTiO_3$ and BIT, in the BIT–$Ba(Ti_{0.99}Mn_{0.01})O_3$ system, the grain growth is enhanced and lead to larger grain size.

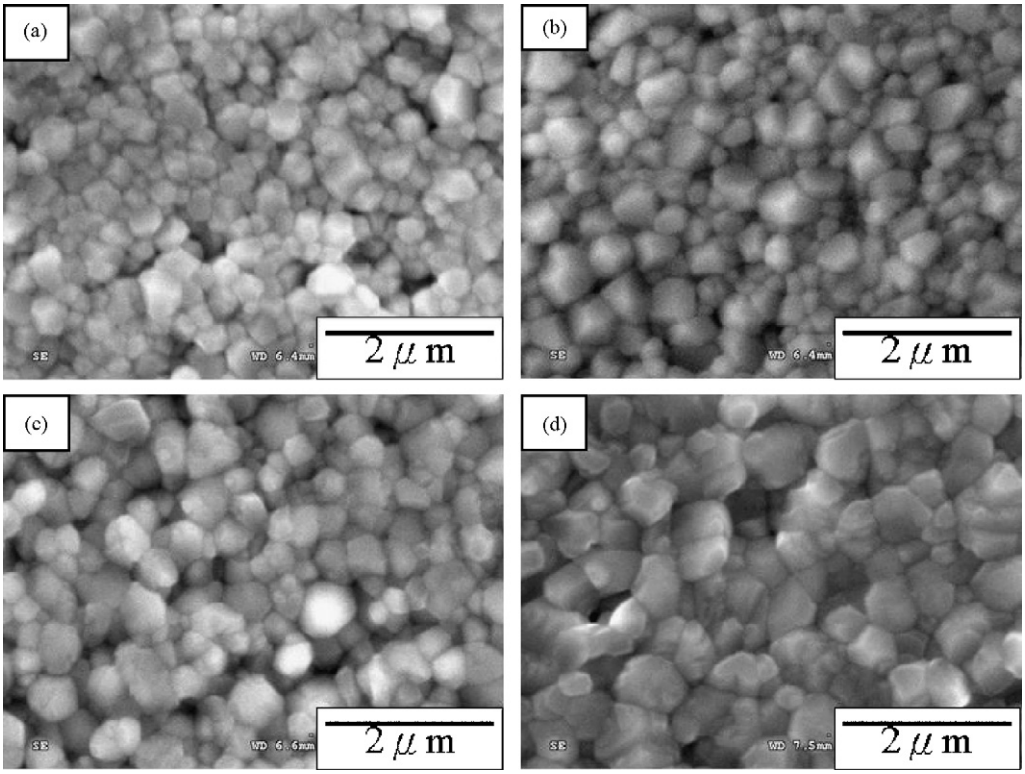

Fig. 4. SEM micrographs of the polished and etched surfaces of the sintered samples doped with various amounts of $Bi_4Ti_3O_{12}$ content: (a) 1 mol%, (b) 2 mol%, (c) 3 mol% and (d) 4 mol%.

Fig. 5 shows the TEM micrographs and the composition analyses in different regions of the sintered samples with (a) 2 mol% BIT and (b) 4 mol% BIT doping. In Fig. 5(a), a ferroelectric domain structure appears near the core of the grain in 2 mol% BIT-doped sample. The composition of this structure was analyzed using EDS. It was found that the Bi and Mn content in the core and shell of the grain had a heterogeneous distribution. Near the shell (A and C points), the concentrations of Bi ions and Mn ions are higher than those near the core (B point). Although Zhang et al.[22] found that Mn ions can suppress the diffusion of Yb into $BaTiO_3$ grains in the $BaTiO_3$–Yb_2O_3–MnO_2 system, resulting in the formation of core–shell structures in the grains, in the BIT–$Ba(Ti_{0.99}Mn_{0.01})O_3$ system, the formation of a core–shell structure is not ascribed to the Mn-suppression. It may be instead related to mass transport of Bi and Mn ions. Although the core–shell structures may be formed by different mechanisms, it is expected that the T_C of the 2 mol% BIT-doped $Ba(Ti_{0.99}Mn_{0.01})O_3$ will shift toward the higher temperature.

For $Ba(Ti_{0.99}Mn_{0.01})O_3$ with 4 mol% BIT, the ferroelectric feature was not found as shown in Fig. 5(b). After analyzing the chemical compositions of the core and shell of the grain, it was found that the concentrations of Bi and Mn ions were nearly identical at positions A, B, and C. The uniform distribution of Bi and Mn ions in the grain indicates the elimination of the core–shell structure. The uniform distribution and high concentration of Bi ions in the grain imply that the forming mechanism of the core–shell structure does not depend on the Mn ion inhibition mentioned above. Comparing Fig. 5(a) and (b), we found that when BIT was added into $Ba(Ti_{0.99}Mn_{0.01})O_3$, the concentration of Mn ion in the grains was diluted due to more Ti ions occupying the B sites of ABO_3; at the same time, the Bi concentration increased in the grains. These two figures show that for the 2 mol% BIT sample, the Bi and Mn ions do not easily diffuse into $BaTiO_3$ and that for the 4 mol% BIT sample, the Bi and Mn ions easily diffuse into $BaTiO_3$, which indicates that the forming mechanism of the core–shell structure in our study is determined by the ion diffusion, i.e. mass transport. Grain growth (Fig. 4) implies that mass transport for the 4 mol% BIT sample is faster than that for the 2 mol% BIT sample. Thus, more BIT enhances the grain growth and leads to the formation of a more homogeneous grain structure. In addition, because of the collapse of the core–shell structure, the T_C of the 4 mol% BIT-doped $Ba(Ti_{0.99}Mn_{0.01})O_3$ is expected to decrease due to a lack of an internal stress between the core and shell.

Fig. 6 shows the DSC curves of $Ba(Ti_{0.99}Mn_{0.01})O_3$ with various amounts of BIT content. When the added BIT content was increased from 0 to 3 mol%, the T_C of $Ba(Ti_{0.99}Mn_{0.01})O_3$ increased from 120 to 133 °C. Again, the increase in T_C is due to the formation of the core–shell structure (Fig. 5). The presence of core–shell structure stabilized the tetragonal phase then raised the ferroelectric transition temperature. With 4 mol% BIT, the T_C dropped to 113 °C, which is consistent with the elimination of the core–shell structure. It was found that the endothermic peak became broad and inconspicuous with more BIT. This result implies that the phase transition from tetragonal to cubic becomes dispersive in a wider range of temperature. It is suggested that the increased T_C and the dispersive phase

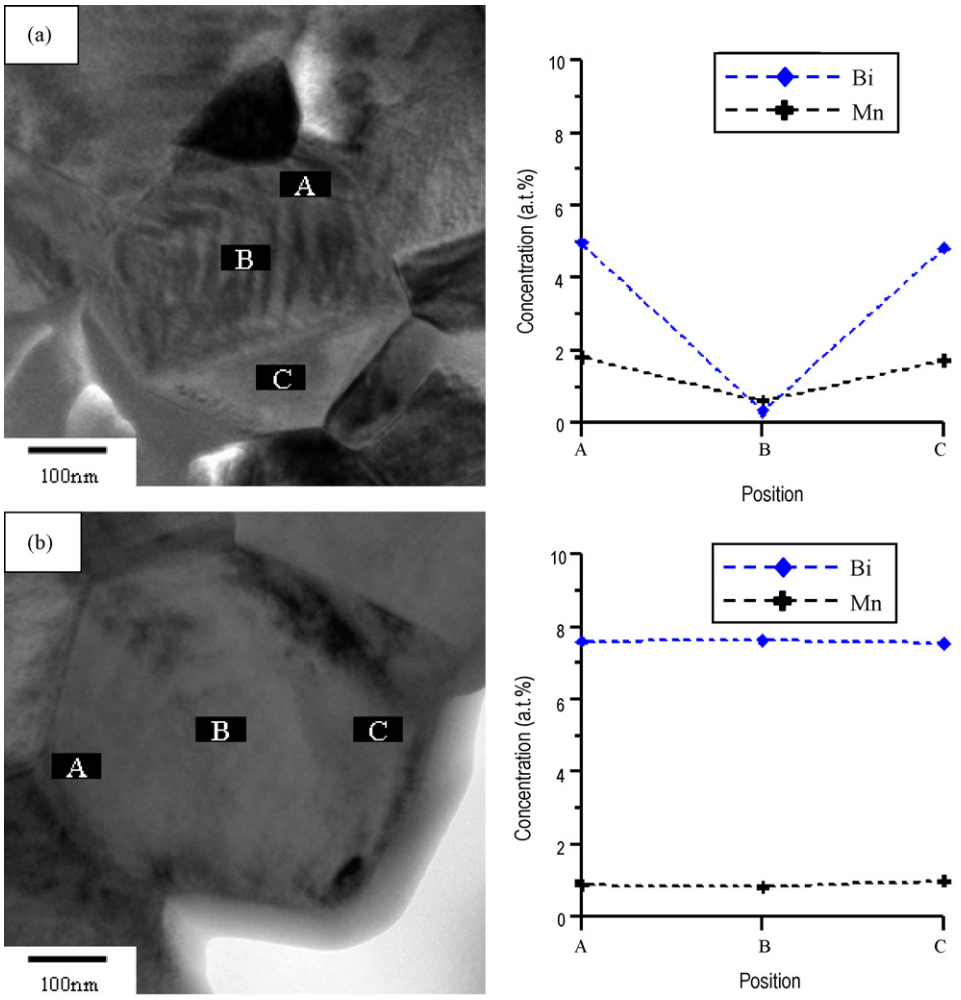

Fig. 5. TEM micrographs of the sintered samples doped with various amounts of $Bi_4Ti_3O_{12}$ content: (a) 2 mol% and (b) 4 mol%.

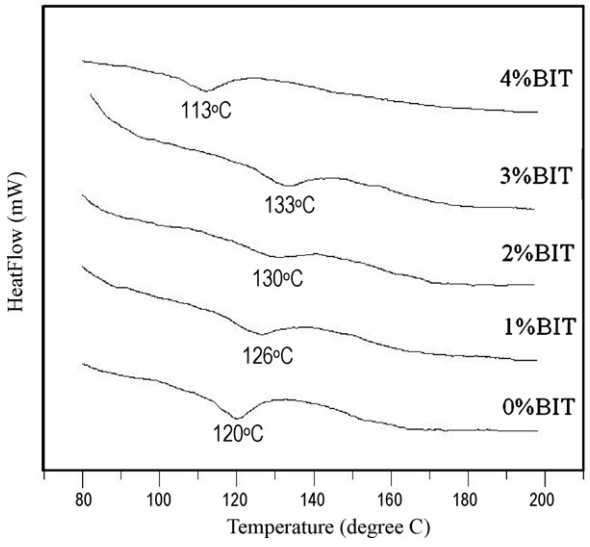

Fig. 6. Differential scanning calorimetry (DSC) curves of $Ba(Ti_{0.99}Mn_{0.01})O_3$ specimens with various amounts of $Bi_4Ti_3O_{12}$ content for the measurement of Curie temperature.

transition greatly contribute to the temperature stability at high temperature.

Fig. 7 shows the temperature dependence of the dielectric constants of the BIT–$Ba(Ti_{0.99}Mn_{0.01})O_3$ system for various amounts of BIT content. It can be observed that the $Ba(Ti_{0.99}Mn_{0.01})O_3$ sample without BIT addition has the highest dielectric constant. When the amount of BIT increased from 0 to 4 mol%, the dielectric constant gradually decreased over the temperature range of −55 to 150 °C. Notably, the sample with 4 mol% BIT had the lowest dielectric constant. It was reported that in the acceptor-doped $BaTiO_3$–Y_2O_3 system, a small grain size may yield higher dielectric constants.[7] The internal stress caused by the mismatch between the core and shell of the grain might be responsible for improving the temperature dependence of the dielectric constant.[23] In Fig. 4, we found that the grain significantly increased from 0.38 to 0.57 μm when the BIT content was increased. Thus, the decreased dielectric constant is attributed to the reduction of grain size which leads to a decrease in the volume ratio of the ferroelectric core to the paraelectric shell region.[24] Due to low tetragonality and a large grain size, 4 mol% BIT-doped $Ba(Ti_{0.99}Mn_{0.01})O_3$ has lower capacitance.

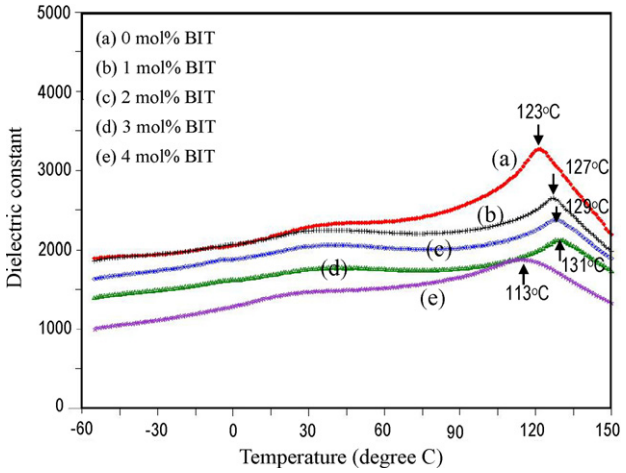

Fig. 7. Temperature dependence of dielectric constant of $Ba(Ti_{0.99}Mn_{0.01})O_3$ specimens with various amounts of $Bi_4Ti_3O_{12}$ content.

From Fig. 7, we can also find T_C. For each sample, there is a peak near 120 °C. The peak temperature value can be defined as the Curie temperature (T_C). In the curves, T_C progressively moves toward higher temperature as the amount of BIT is increased up to 3 mol%. The T_C of the samples with 0, 1, 2, and 3 mol% BIT are 123, 127, 129, and 131 °C, respectively. When the BIT content was further increased to 4 mol%, the T_C declined to 113 °C, which is lower than that of the pure $Ba(Ti_{0.99}Mn_{0.01})O_3$ sample. The total trend is consistent with the results of DSC in Fig. 6. As mentioned above, the core–shell structure consisting of a ferroelectric un-reacted core and a paraelectric reacted shell results in a small internal stress, which inhibits the phase transition from tetragonal to cubic. The lowest T_C was caused by the collapse of the core–shell structure (Fig. 5).

Fig. 8 shows the TCC curves for $Ba(Ti_{0.99}Mn_{0.01})O_3$ specimens as a function of the BIT content over the temperature range of −55 to 150 °C. The variation of capacitance decreased when BIT content increased from 0 to 2 mol% and then increased

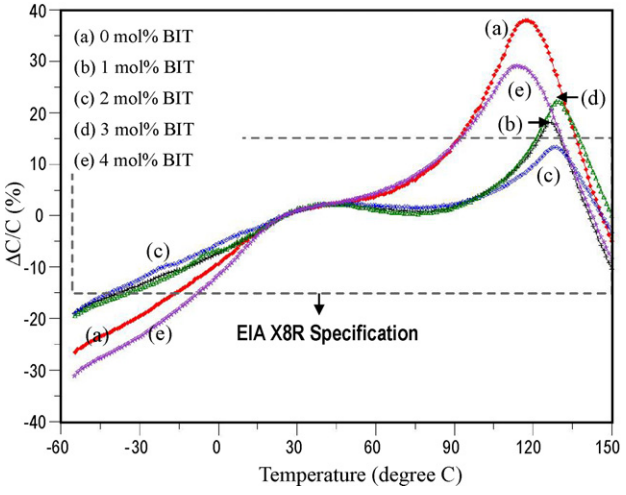

Fig. 8. Temperature coefficient of capacitance (TCC) of $Ba(Ti_{0.99}Mn_{0.01})O_3$ specimens as a function of the $Bi_4Ti_3O_{12}$ content.

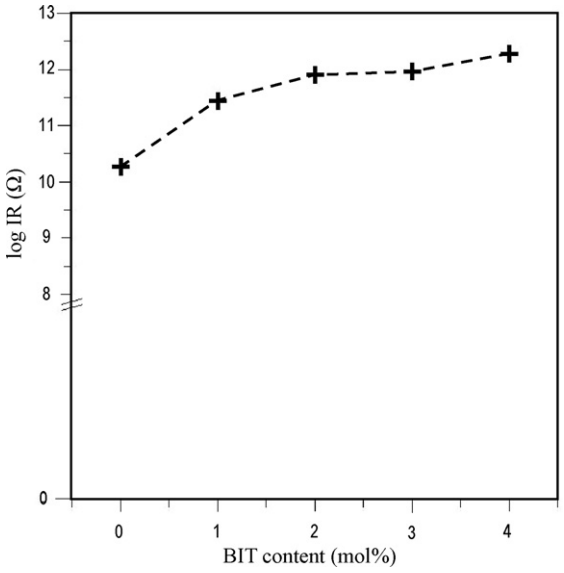

Fig. 9. Insulation resistance (IR) of $Ba(Ti_{0.99}Mn_{0.01})O_3$ specimens as a function of the $Bi_4Ti_3O_{12}$ content.

from 2 to 4 mol%. Because of the internal stress resulting from the mismatch between core and shell regions, the T_C increased and the temperature stability of capacitance was enhanced. The temperature characteristics of capacitance for the sample with 2 mol% BIT is very close to the X8R specification. It shows less than 5% variation of the dielectric constant at a temperature of 150 °C. However, the variation of dielectric constant at a temperature of −55 °C was around −20%. This fails to satisfy the EIA X8R temperature characteristic specification, which is indicated by a dashed line rectangle shape in Fig. 8. It has been reported that the curve of capacitance variation at higher temperature sites will be shifted toward the negative direction, which is called the "clockwise effect", as the dielectric thickness becomes thinner for MLCC applications.[25] When more than 3 mol% BIT was added to $Ba(Ti_{0.99}Mn_{0.01})O_3$, the variation of capacitance became too large to satisfy the X8R specification. This is perhaps caused by the coarser grain size with a more indefinite core/shell structure. Fig. 9 shows the insulation resistance (IR) of $Ba(Ti_{0.99}Mn_{0.01})O_3$ ceramics for various amounts of BIT content. It was found that the insulation resistance increased with increasing $Bi_4Ti_3O_{12}$ content and the IRs of all samples were larger than 100 GΩ after adding BIT into $Ba(Ti_{0.99}Mn_{0.01})O_3$. It can be concluded that the ceramic material has great potential for the use in EIA X8R-type MLCCs.

4. Conclusions

There was no secondary phase when the $Bi_4Ti_3O_{12}$ content was below 4 mol%. This indicates that $Bi_4Ti_3O_{12}$ dissolved into the $BaTiO_3$ perovskite lattice, leading to a contraction of the unit cell volume.

The grain size was significantly enhanced by increasing the $Bi_4Ti_3O_{12}$ content. The sintering temperature of $Ba(Ti_{0.99}Mn_{0.01})O_3$ ceramics could be reduced to 1200 °C by doping them with more than 1 mol% $Bi_4Ti_3O_{12}$.

Tetragonality increased when the $Bi_4Ti_3O_{12}$ content was increased from 0 to 2 mol% and then decreased from 2 to 4 mol%. This is consistent with the TEM results in which the core–shell structure was observed with 2 mol% $Bi_4Ti_3O_{12}$ but was destroyed when the $Bi_4Ti_3O_{12}$ content was increased to 4 mol%.

The Curie point shifted to a higher temperature, from 123 to 131 °C, when the $Bi_4Ti_3O_{12}$ content was increased from 0 to 3 mol%, and dropped to 113 °C when the content was 4 mol%. The 3 mol% $Bi_4Ti_3O_{12}$ sample has the highest Curie temperature. The trend was caused by the change of the core–shell grain structure.

The temperature characteristics of capacitance at a temperature of 150 °C was less than 5% when 2 mol% $Bi_4Ti_3O_{12}$ was added. However, the variation of the dielectric constant at a temperature of −55 °C was around −20%. Due to the "clockwise effect", ceramic materials have great potential as EIA X8R-type multilayer ceramic capacitors.

Acknowledgment

The authors would like to thank Darfon Electronics Corps for their financial and technical support.

References

1. Syamaprasad, U., Galgali, R. K. and Mohanty, B. C., Dielectric properties of the $Ba_{1-x}Sr_xTiO_3$ system. *Mater. Lett.*, 1988, **7**, 197–200.
2. Hshie, H. L. and Fung, T. T., Effect of green states on sintering behavior and microstructural evolution of high-purity barium titanate. *J. Am. Ceram. Soc.*, 1990, **73**, 1566–1573.
3. Okino, Y., Shizuno, H., Kusumi, S. and Kishi, H., Dielectric properties of rare-earth-oxide-doped $BaTiO_3$ ceramics fired in reducing atmosphere. *Jpn. J. Appl. Phys.*, 1994, **33**, 5393–5396.
4. Na, E., Choi, S. C. and Paik, U., Temperature dependence of dielectric properties of rare-earth element doped $BaTiO_3$. *J. Ceram. Proc. Res.*, 2003, **4**, 181–184.
5. Jung, Y. S., Na, E. S., Paik, U. Y., Lee, J. H. and Kim, J. H., A study on the phase transition and characteristics of rare earth element doped $BaTiO_3$. *Mater. Res. Bull.*, 2002, **37**, 1633–1640.
6. Wang, S., Zhang, S., Zhou, X., Li, B. and Chen, Z., Effect of sintering atmospheres on the microstructure and dielectric properties of Yb/Mg co-doped $BaTiO_3$ ceramics. *Mater. Lett.*, 2005, **59**, 2457–2460.
7. Song, Y. H., Hwang, J. H. and Han, Y. H., Effects of Y_2O_3 on temperature stability of acceptor-doped $BaTiO_3$. *Jpn. J. Appl. Phys.*, 2005, **44**, 1310–1313.
8. Song, Y. H. and Han, Y. H., Effects of rare-earth oxides on temperature stability of acceptor-doped $BaTiO_3$. *Jpn. J. Appl. Phys.*, 2005, **44**, 6143–6147.
9. Hwang, J. H., Choi, S. K. and Han, Y. H., Dielectric properties of $BaTiO_3$ codoped with Er_2O_3 and MgO. *Jpn. J. Appl. Phys.*, 2001, **40**, 4952–4955.
10. Li, Y., Yao, X. and Zhang, L. Y., High permittivity neodymium-doped barium titanate sintered in pure nitrogen. *Ceram. Int.*, 2004, **30**, 1325–1328.
11. Lin, T. F., Hu, C. T. and Lin, I. N., Influence of stoichiometry on the microstructure and positive temperature coefficient of resistivity of semiconducting barium titanate ceramics. *J. Am. Ceram. Soc.*, 1990, **73**, 531–536.
12. Chen, J., Jin, W. and Yao, Y., Study of the anomalous grain growth of $BaTiO_3$ ceramics. *Ferroelectrics*, 1993, **142**, 153–159.
13. Hiruma, Y., Aoyagi, R., Nagata, H. and Takenaka, T., Piezoelectric properties of $BaTiO_3$–$(Bi_{1/2}K_{1/2})TiO_3$ ferroelectric ceramics. *Jpn. J. Appl. Phys.*, 2004, **43**, 7556–7559.
14. Takeda, H., Aoto, W. and Shiosaki, T., $BaTiO_3$–$(Bi_{1/2}Na_{1/2})TiO_3$ solid-solution semiconducting ceramics with $T_C > 130$ °C. *Appl. Phys. Lett.*, 2005, **87**, 102104.
15. M'Peko, J. C., Portelles, J. and Rodriguez, G., Densification process of $BaTiO_3$ containing $Bi_4Ti_3O_{12}$. *J. Mater. Sci. Lett.*, 1997, **16**, 1850–1852.
16. Billegas, M., Moureoure, C., Fernandez, J. F. and Duren, P., Preparation and sintering behavior of submicronic $Bi_4Ti_3O_{12}$ powders. *J. Mater. Sci.*, 1996, **31**, 949–959.
17. Kishi, H., Mizuno, Y. and Chozono, H., Base-metal electrode-multilayer ceramic capacitors: past, present and future perspectives. *Jpn. J. Appl. Phys.*, 2003, **42**, 1–15.
18. Li, T., Li, L., Zhao, J. and Gui, Z., Modulation effect of Mn^{2+} on dielectric properties of $BaTiO_3$-based X7R materials. *Mater. Lett.*, 2000, **44**, 1–5.
19. Holland, T. J. B. and Redfern, S. A. T., Unit cell refinement from powder diffraction data; the use of regression diagnostics. *Mineral. Mag.*, 1997, **61**, 65–77.
20. Yang, K. Y., Wang, J. W. and Fung, K. Z., Roles of lithium ions and La/Li-site vacancies in sinterability and total ionic conduction properties of polycrystalline $Li_{3x}La_{2/3-x}TiO_3$ solid electrolytes ($0.21 \leq 3x \leq 0.50$). *J. Alloys Compd.*, 2008, **458**, 415–424.
21. Yamaoka, N., Fukui, M. and Nakamura, H., Low temperature sintered $BaTiO_3$ ceramics with $Bi_4Ti_3O_{12}$ added. *Jpn. J. Appl. Phys.*, 1981, **20**(4), 139–142.
22. Zhang, S., Wang, S., Zhou, X., Li, B. and Chen, Z., Influence of 3d-elements on dielectric properties of $BaTiO_3$ ceramics. *J. Mater. Sci. Mater. Electron.*, 2005, **16**, 669–672.
23. Armstrong, T. R. and Buchanan, R. C., Influence of core–shell grains on the internal stress state and permittivity response of zirconia-modified barium titanate. *J. Am. Ceram. Soc.*, 1990, **73**, 1268–1273.
24. Takeuchi, T., Ado, K., Asai, T., Kageyama, H., Saito, Y., Masquelier, C. and Nakamura, O., Thickness of cubic surface phase on barium titanate single-crystalline grains. *J. Am. Ceram. Soc.*, 1994, **77**, 1665–1668.
25. Kobayashi, H., *et al.*, Dielectric ceramic composition and electronic device, TDK Corporation, United States Patent 6764,976, 2002.